444

Soil moisture retrieval during the Southern Great Plains Hydrology Experiment 1999: A comparison between experimental remote sensing data and operational products

Matthias Drusch, Eric F. Wood[1], Huilin Gao[1] and Ariane Thiele[2]

Research Department

[1] Dept. of Civil and Environmental Engineering, Princeton University, NJ, USA

[2] Meteorologisches Institut der Universität Bonn, Germany

June 2004

Also published in *Water Resources Res.*, 40, 2004 W02504, doi:10.1029/2003WR002441,

The Library
ECMWF
Shinfield Park
Reading, Berks RG2 9AX

library@ecmwf.int

Series: ECMWF Technical Memoranda

A full list of ECMWF Publications can be found on our web site under:
http://www.ecmwf.int/publications.html

Abstract

Soil moisture images for the Southern Great Plains Hydrology Experiment (SGP99) were derived from airborne passive microwave measurements obtained from the Electronically Scanned Thinned Array Radiometer (ESTAR) and the Polarimetric Scanning Radiometer (PSR) at L-band and C-band, respectively. In order to mimic operational products, a robust retrieval method is chosen and the corrections for vegetation and surface roughness are based on average values from the literature. Validation against field measurements results in rms errors and biases of 2.9 % and 4.2 % in volumetric soil moisture for the ESTAR data set and 4.6 % and 6.0 % for the PSR product. For this sparsely vegetated experiment region, the quality of the C-band derived soil moisture is therefore comparable to the corresponding L-band product. The accuracies of the operational data sets, namely the European Centre for Medium-range Weather Forecasts (ECMWF) 40 year re-analysis product (ERA40) and the European Remote Sensing Satellite (ERS) scatterometer derived soil moisture, are quantified based on the high resolution PSR soil moisture images for the SGP99 region. The ERA40 re-analysis comprises soil moisture data for four soil layers at the T159 spectral resolution. The top 7 cm layer soil moisture product is in reasonable agreement with the C-band derived soil moisture data sets. Temporal and spatial patterns are well represented but a significant wet bias of up to 14.4 % (ERA40) is present in dry conditions. In order to evaluate the quality of the operational data sets on a longer temporal time scale, in-situ soil moisture measurements at the Little Washita NOAA/ATDD (National Oceanic and Atmospheric Administration / Atmospheric Turbulence and Diffusion Division) site are used to analyze time series for June 1997 to December 1998. The temporal evolution of soil moisture is captured reasonably well by the ERA40 product and the ERS scatterometer derived surface soil moisture data set. RMS errors were found to be 5.6 % and 5.7 %, respectively. The study shows that passive microwave remote sensing has the potential to improve operational products.

1. Introduction

Numerous studies show the impact of surface soil moisture on the terrestrial water and energy budgets. For regional to global scale applications in hydrological and atmospheric modeling, remote sensing techniques have to be applied to derive soil moisture fields with sufficient spatial and temporal coverage. Measurements at L-band frequencies, which would be best suited for soil moisture retrievals since the effects of the atmosphere and the vegetation are small, will not be available before 2006 (Kerr et al. [2001]). However, satellite-borne instruments at C-band, the Advanced Microwave Scanning Radiometer-Eos (AMSR-E, launched in May 2002), AMSR (launched in December 2002), and the ERS scatterometer have the capability to obtain measurements, which can be related to surface soil moisture. From the ERS satellites wind scatterometer data have been available for roughly a decade. Recently, a global data set of a soil water index was derived from these active microwave measurements (Wagner and Scipal [2000], Wagner et al. [1999], Wagner [1998]) as a secondary product.

In order to evaluate the potential of C-band measurements for data assimilation applications experimental data from the SGP99 experiment are compared to operational soil moisture data sets. The operational data sets comprise ERS scatterometer data and the ERA40 re-analysis product derived at ECMWF. The experimental high resolution data sets are PSR C-band data and L-band measurements from ESTAR. The PSR instrument mimics AMSR measurements with respect to the frequency and the viewing angle.

The spatial and temporal variability of surface soil moisture is high. Therefore, it is difficult to compare data sets with different resolutions. Field experiments at the regional scale, which comprise airborne remote sensing data, are best suited to bridge the scales from in-situ point measurements to model results at resolutions of up to 150 km. In the first part of this paper, we focus on the derivation of high resolution soil moisture fields from airborne passive microwave measurements at L-band and C-band. A robust retrieval method (Jackson et al. [1999]) and surface data, which will be available operationally in the future, are used.

The airborne data sets are validated against in-situ observations to define the absolute accuracy of both products. Since L-band measurements are considered to be the ideal frequency for soil moisture remote sensing the C-band data sets derived from PSR are compared to the ESTAR soil moisture product to obtain a relative measure of the errors.

The second part of the paper shows a comparison between the PSR high resolution data set and the operational products. The PSR soil moisture data are linearly averaged to a 0.25° grid. The ERA40 re-analysis and the ERS product are interpolated to the corresponding resolution. In order to evaluate the operational products on a larger temporal scale, section 5 gives a comparison with soil moisture measurements taken at Tilden Meyers NOAA/ATDD station in the Little Washita area during the period of June 1997 to December 1998.

2. Experimental Soil Moisture Data Sets

The SGP99 experiment covered the period from July 8 to July 20 1999. A comprehensive description of the experiment is available under http://hydrolab.arsusda.gov/sgp99/sgp99b.htm. One major rainfall event during the night of July 9 and the early morning of July 10 caused a significant increase in soil moisture in the entire SGP region, followed by a dry down period until the end of the experiment. The amounts of rainfall varied from up to 107 mm at the very centre of the storm located in the El Reno (ER) area, ~40 mm in the northern experiment area around the Central Facility (CF) to 10-40 mm in the Little Washita (LW) area in the south. In addition, the western part of the SGP99 study area (as defined by the airborne remote sensing flight lines) was drier than the eastern part with the minimum in the very south west (Fig. 1).

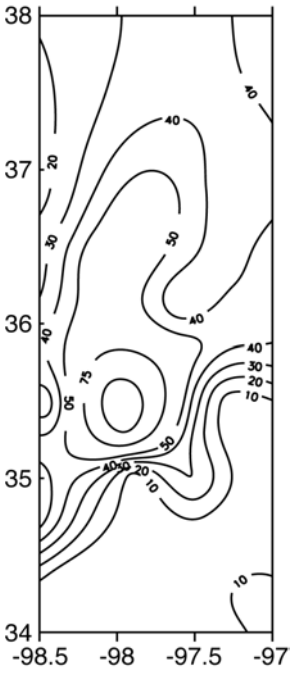

Figure 1 Accumulated rainfall in mm for July 9 and July 10

Gravimetric soil moisture for the top 5 cm layer was sampled during the morning hours on twenty-two (LW), six (ER) and five (CF) fields. In general, fourteen samples were taken on each field to capture the spatial variability. Volumetric soil moisture was inferred from gravimetric soil moisture and bulk density, which was measured once for every field. Based on these measurements, daily averages of volumetric soil moisture were computed for the three study areas. Figure 2 shows time series of the gravimetric soil moisture

measurements of the top 5 cm layer. Maximum values for the LW, ER and CF are 0.20, 0.27 and 0.44, respectively.

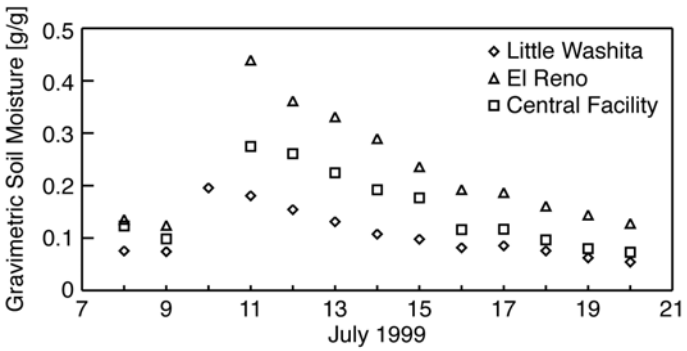

Figure 2 Temporal evolution of gravimetric soil moisture for the top 0-5cm soil layer (daily averages for the Little Washita (LW), El Reno (ER) and Central Facility (CF) areas).

2.1 Soil Moisture Retrieval Algorithm for ESTAR and PSR

The theory for passive microwave radiative transfer at L- and C-band is well understood and has been applied for several decades now. Most of the existing retrieval algorithms are based on a solution of the scalar radiative transfer equation (e.g. Kerr and Njoku [1990]):

$$T_{bv} = T_{au} + e^{-\tau_{at}}(T_{ad} + T_{sky}e^{-\tau_{at}})(1-\varepsilon)e^{-2\tau^*} + e^{-\tau_{at}}\left[\varepsilon T_s e^{-\tau^*} + T_V(1-\omega^*)(1-e^{-\tau^*})(1+(1-\varepsilon)e^{-\tau^*})\right] \quad (1)$$

where T_{bv} is the brightness temperature for vegetated surfaces, T_{au} and T_{ad} are the upward and downward contributions from the atmosphere, T_s is the effective soil temperature, T_v the vegetation temperature, T_{sky} the cosmic radiation, ε the rough soil emissivity and ω^* the single scattering albedo (Joseph et al. [1976]). τ_{at} and τ^* are the optical depth of the atmosphere and the effective optical depth of the vegetation, respectively. This solution is strictly valid for homogeneous areas only. However, since there are hardly any aggregation effects caused by non-linearities in radiative transfer and land surface heterogeneity for L-band and C-band in sparsely vegetated areas (Drusch et al. [1999], Crow et al. [2001]), linear averages can be used in the retrieval. Polarization dependency is omitted in Equation (1) since this study is based on horizontally polarized measurements only. Under the assumptions that the single scattering albedo of the vegetation is zero, the atmospheric up- and down-welling contributions to the brightness temperature measured at aircraft height are zero and the temperature of the vegetation is equal to the effective soil temperature, Equation (1) can be simplified and soil moisture can be inferred in a four step algorithm based on the surface emissivity ε_{surf} (Jackson et al. [1982]):

$$\frac{T_b}{T_s} = \varepsilon_{surf} = 1 + (\varepsilon - 1)e^{-2\tau^*} \quad (2)$$

This approximation is valid for low frequency measurements and for the specific conditions prevailing in the SGP area (Jackson et al. [1982]). The algorithm is described in detail in Jackson et al. [1995] and was used in previous SGP studies (Jackson et al. [1999], Jackson et al. [2001]). For the sake of a better understanding we will briefly summarize the four steps of the algorithm.

In the first step surface emissivity is calculated by dividing measured brightness temperatures by the corresponding effective soil temperature (Equation 2). The effective temperature can be parameterized using

surface temperature and soil temperature following Choudhury et al. [1982]. Surface emissivity is then corrected for attenuation effects due to vegetation to derive the rough soil emissivity ε:

$$\varepsilon = 1 + (\varepsilon_{surf} - 1)e^{2 \times b \times vwc / \cos\theta} \quad (3)$$

In this study, the optical depth of vegetation is obtained from the vegetation water content *wvc*, incident angle θ and the vegetation parameter *b*, which is frequency dependent (e.g. Jackson and Schmugge [1991]). In the third step, specular soil emissivity ε_{spec} is calculated by applying a roughness correction based on the roughness parameter h (Choudhury et al. [1979]):

$$\varepsilon_{spec} = 1 + (\varepsilon - 1)e^{h} \quad (4)$$

Finally, the specular emissivity is converted to soil moisture by inverting the dielectric mixing model published by Wang and Schmugge [1980]. The soil moisture retrievals for the L- and C-band measurements from ESTAR and PSR, respectively, are based on actual measurements of the underlying vegetation and soil parameters. The corresponding data sets are introduced in sections 2.2 and 2.3.

2.2 ESTAR L-band Measurements

During the last decade several field experiments in the Southern Great Planes have been performed (e.g. Jackson et al. [1999], Jackson et al. [1995]). Airborne ESTAR measurements revealed an impressive potential for surface soil moisture retrievals and a number of reviewed publications are related to L-band derived soil moisture (e.g. Jackson et al. [1999], Drusch et al. [1999], Bindlish et al. [2001], Margulis et al. [2002]). For a general description of the instrument the reader is referred to Le Vine et al. [1994]. The calibration of the radiometer and the mapping procedure, which produces brightness temperatures on a 0.05° grid, is outlined in Le Vine et al. [2001]. A first comparison between brightness temperatures and soil moisture is given in that paper as well. However, Le Vine et al. [2001] conclude that a more detailed analysis would be necessary to actually derive spatially distributed soil moisture data from the measurements. The closest date of measurements to the only rainfall event on July 9 / 10 is July 14. Therefore, the dynamic range of soil moisture is quite small. A total of 6 days (07/08, 07/09, 07/14, 07/15, 07/19, 07/20) of ESTAR measurements is available.

To normalize brightness temperature in Equation (2), effective soil temperature was computed from 2 m air and 30 cm soil temperature obtained at the Oklahoma Mesonet stations (Choudhury et al. [1982]). Values at the stations were interpolated to the 0.05° grid as defined by the ESTAR data sets using thin plate splines (Barrodale et al. [1993], Powell [1992]). This temperature data set does not capture the full spatial variability of a true high resolution product. However, in operational applications the temperature field will be obtained either through infrared observations, in-situ measurements, model data or combinations of these three data sources. Therefore, an operational effective soil temperature field will be smoothed as well and hardly represent small scale variations properly. The use of air temperature instead of surface temperature may result in slightly higher emissivities (Jackson et al. [2002]).

Vegetation effects are corrected using area averages of vegetation water content for Little Washita, El Reno and Central Facility. Measurements of this quantity were taken once during the experiment period. Data from twenty, three and five individual sites, respectively, were processed. In order to demonstrate the potential for operational applications the plant parameter *b* and the roughness parameter *h* were not calibrated to the SGP99 data set or the individual sites. Average values as reported in the reviewed literature were assigned.

For b a value of 0.1 was found to be typical for various vegetations types (legumes, small grains and corn) at 1.4 GHz (Schmugge and Jackson [1992]).

The roughness correction after Choudhury et al. [1979] results in the specular reflectivity of the surface. In Equation (4) the roughness parameter *h* was set to 0.3. This value represents a medium rough surface (Table 3 in Choudhury et al. [1979]). Depending on the land cover classification h values of either 0.1 or 0.2 were found for the SGP97 experiment (Jackson et al. [1999]). The corresponding *b* parameter for that study varied between 0.085 and 0.119. It may well be that these values are more appropriate for the specific sites or vegetation types. However, in operational large scale applications this type of information will not always be available and the soil moisture retrievals will have to rely on average parameters from the literature.

The relationship between volumetric soil moisture and the specular surface reflectivity is described by the Fresnel equation and the dielectric constant of the soil as computed from the dielectric mixing model by Wang and Schmugge [1980]. Based on soil textures (fractions of sand and clay), which are taken from the STATSGO (State Soil Geographic) Data Base (Jackson et al. [1999]), and soil bulk densities, which were measured during the experiment at the individual sites, the dielectric mixing model can be inverted to compute the volumetric soil water content.

In order to ensure maximum comparability with results from the SGP97 experiment (Jackson et al. [1999]) area averages of volumetric soil moisture are analyzed on a daily basis. The comparison between ESTAR derived soil moisture and in-situ measurements for the three main study areas as described in section 2 results in an rms error of ~ 4 % in volumetric soil moisture (Fig. 3). When the bias is subtracted in the rms calculation a value of 3 % is obtained (rms-b). A similar value was obtained for the L-band derived soil moisture data in the SGP97 study (Jackson et al. [1999]). This random error can be caused by uncertainties in the geophysical parameters, e.g. temporally constant vegetation water content, approximations in the

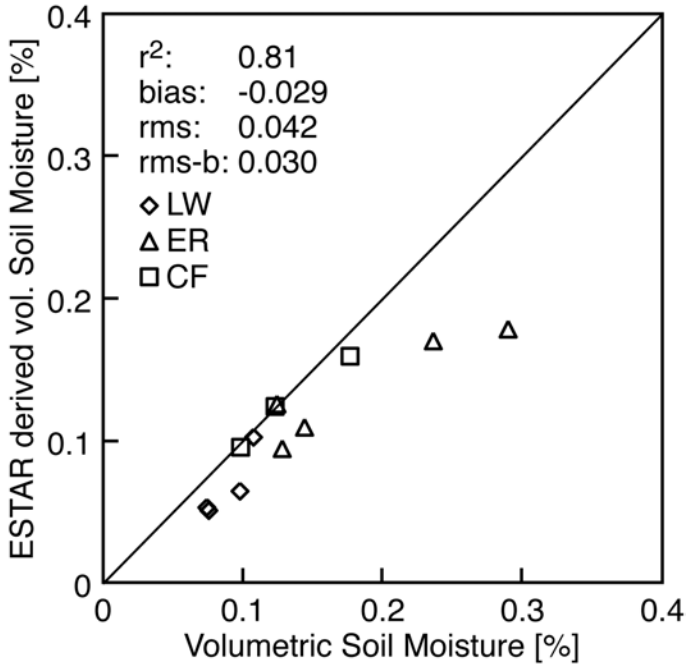

Figure 3 Comparison between daily averaged volumetric soil moisture from in-situ observations and ESTAR derived soil moisture for the three experiment areas (for the rms-b calculation the bias was subtracted).

retrieval algorithm, e.g. no difference between vegetation and effective soil temperature, and the uncertainty in the ground truth data. Comparisons on the field scale show higher rms errors, since the difference in the spatial resolution of the airborne data and the in-situ measurements is larger. However, the focus on future operational applications justifies the aggregation to area means. The bias of -2.9 % is entirely due to the choice of the *h* and *b* parameters. Calibration to regional values, which may be possible in some operational applications, e.g. re-analysis projects, can reduce systematic errors. For LW and CF no soil moisture values could be retrieved for July 19 and July 20. On both days the soil was extremely dry at both sites and the inversion of the dielectric mixing model was numerically impossible. Due to incomplete spatial coverage no data are available for July 14 for the ER and CF areas. However, with an r^2 of 0.81 the potential of L-band radiometers for soil moisture retrievals is demonstrated.

Soil moisture images at 0.05° resolution were then derived using the retrieval algorithm as described above. ESTAR brightness temperatures and effective soil temperature from Mesonet observations were used to derive surface emissivity. The vegetation water content data set for the experiment region is based on the field measurements and the NDVI (Normalized Difference Vegetation Index) computed from Landsat TM (Thematic Mapper) (Jackson et al. [2002]). *b* and *h* parameters remained constant in time and space. Soil textures were taken from the STATSGO Data Base. A map of bulk densities, which is available through the SGP99 data base, was produced from the individual field measurements and a Landsat TM derived land cover classification. In order to avoid numerical problems in the inversion of the dielectric mixing model a minimum value of the real part of the dielectric constant of the soil of 2.0 was assumed for very dry conditions.

2.3 PSR C-band Measurements

The Polarimetric Scanning Radiometer PSR was evaluated the first time during SGP99. A detailed study on the instrument and the calibration is given in Jackson et al. [2002]. Data from the 7.325 GHz channel were processed since this frequency seemed to be least affected by anthropogenic radio frequency interference (RFI) (Jackson et al. [2002]). The SGP99 study area was mapped on 6 days (07/08, 07/09, 07/11, 07/14, 07/19). In order to compare ESTAR and PSR data, the PSR brightness temperatures were linearly sampled to a 0.05° resolution.

The soil moisture analysis presented by Jackson et al. [2002] already reveals the significant potential of C-band measurements. In contrast to that study, we present the same robust approach as outlined in section 2.1, which is based on constant *h* and *b* parameters from the literature. A comparison with the L-band derived soil moisture, which is regarded as the 'optimal' soil moisture product, is presented in section 2.4.

The soil moisture retrieval for the CF, ER and LW areas was performed using the same data sets for effective soil temperature, vegetation water content, sand and clay fraction and soil bulk density as for the ESTAR soil moisture retrieval. Since the *b* parameter is strongly frequency dependent a value of 0.5 is assigned following Schmugge and Jackson [1992]. The *b* parameters chosen for the ESTAR and PSR retrievals were derived from the same data sets and are therefore consistent. The *h* parameter in the roughness parameterization used in this study is insensitive to wavelength. Choudhury et al. [1979] show that measurements over an agricultural area near Phoenix yield to an h parameter of 0.6 for wavelengths of 1.55 and 21 cm. They conclude that: '… the fact that *h* does not scale with wavelength is indicative of the shortcomings of the model (page 5705, Choudhury et al. [1979])'. However, since roughness seems to be undefined on large scales and appropriate data are not available this parameterization has been used widely. Consequently, a constant value of 0.3 is used for the PSR soil moisture retrieval presented in this paper.

The comparison with volumetric soil moisture obtained from the field measurements are shown in Fig. 4. Bias, rms and rms-b error were found to be 4.6 %, 6 % and 3.8 %, respectively. These values are slightly larger than the errors of the ESTAR derived soil moisture. However, since ESTAR and PSR data sets do not comprise exactly the same dates and since the number of observations is small it can not be concluded that ESTAR yields significantly better results. The slightly higher r^2 value of 0.86 for the PSR data is due to the fact that the dynamic range of soil moisture is higher than in the ESTAR observations.

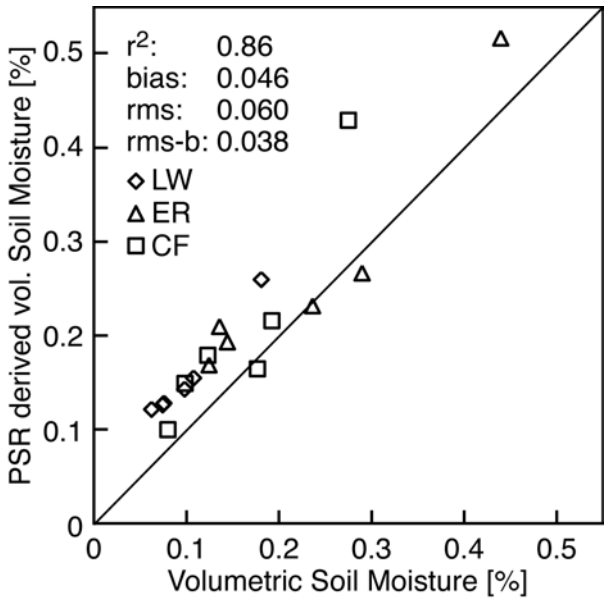

Figure 4 Comparison between volumetric soil moisture from in-situ observations and PSR derived soil moisture (daily area averages).

Soil moisture images derived from PSR measurements are shown in Fig. 5. Again, the *h* and *b* parameters were kept constant at values of 0.3 and 0.5, respectively. Temperature, vegetation and soil data sets are identical to those used for the ESTAR soil moisture retrieval. The images are generally in very good agreement with the results presented in Jackson et al. [2002]. The meteorological conditions are well represented in the temporal and spatially consistent patterns.

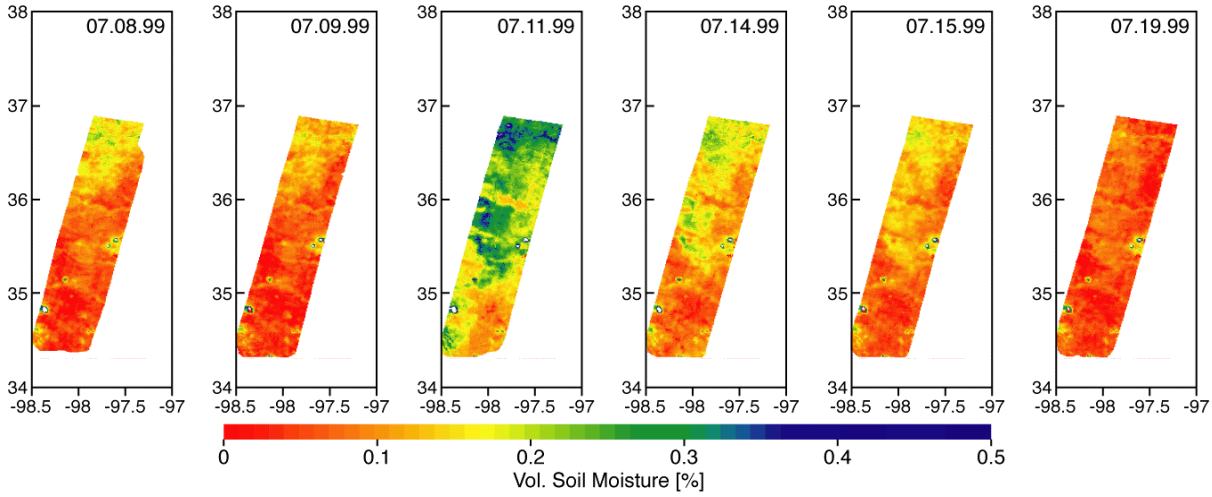

Figure 5 PSR derived soil moisture maps for the SGP99 experiment.

2.4 PSR vs. ESTAR

The comparisons between ESTAR and PSR derived soil moisture and the in-situ measurements indicate that the 7.3 GHZ PSR data have a high potential for soil moisture retrievals. However, the errors presented in the previous sections are based on average values for three areas and four to six days, depending on the specific area. The error on the regional scale can be quantified comparing PSR and ESTAR derived soil moisture maps on a daily basis. In order to mimic operational products the high resolution soil moisture maps are aggregated linearly to a 0.25° grid. In addition, this procedure minimizes errors caused by different radiometer resolutions, geo-location of the raw radiometer observations and mapping to the regular grids.

Scatter diagrams for the five experiment days when both radiometers were operated are shown in Fig. 6. The values for r² range from 0.82 to 0.45. High correlations are obtained for scenes with high spatial gradients in soil moisture. Low values for r^2 are obtained in dry conditions with almost uniform soil moisture distributions. The rms errors vary between 1.9 % and 4.8 %, which is comparable to the errors resulting from comparisons with the in-situ measurements. When compared to in-situ measurements, ESTAR derived soil moisture was biased low while PSR was biased high. In this comparison, the ESTAR soil moisture data show systematically higher values than the PSR data set in four out of five cases. Although these differences are comparably small, it can be concluded that even a perfect adjustment or calibration to field measurements will not ensure bias-free soil moisture fields on the regional scale even if the fields were distributed over the entire study region. However, this comparison shows that passive microwave C-band measurements have a similar potential for soil moisture retrieval as L-band observations in sparsely vegetated areas when no strong RFI is present.

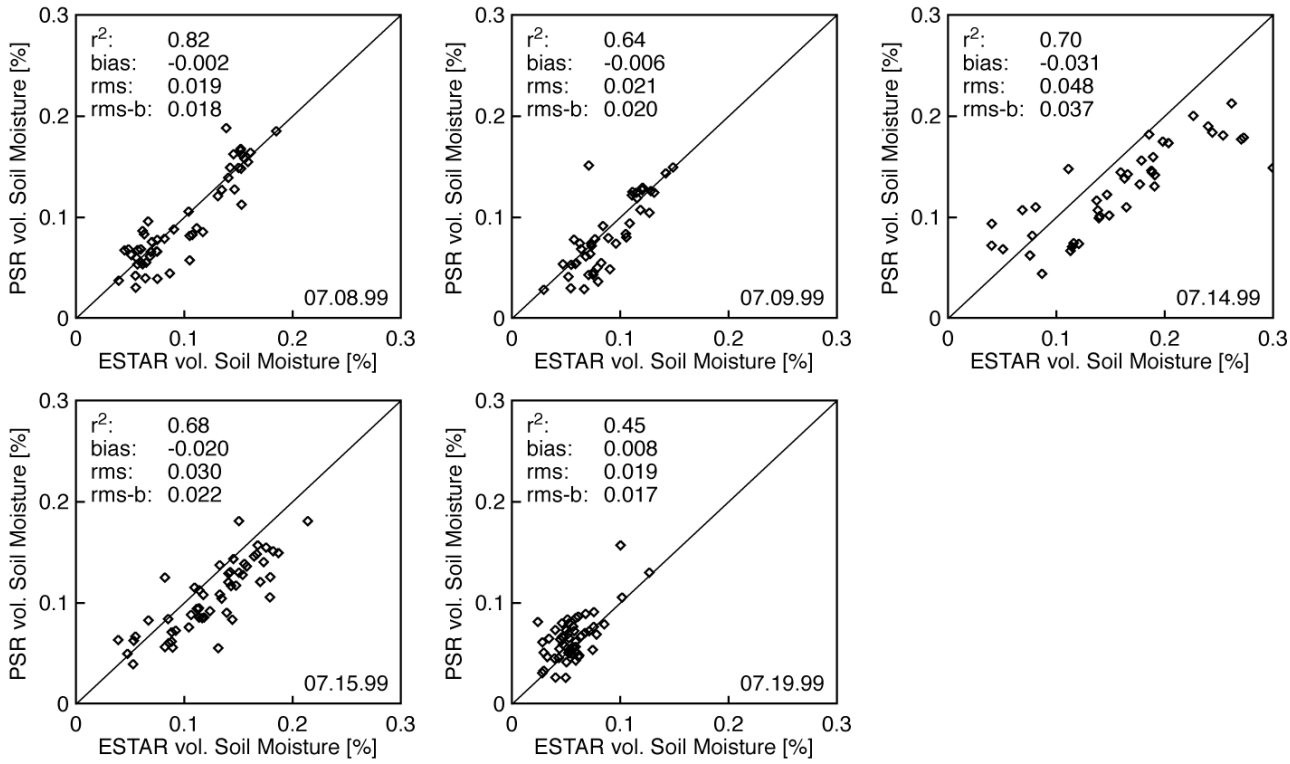

Figure 6 Comparison between volumetric soil moisture derived from ESTAR brightness temperatures and the PSR derived soil moisture. Data are aggregated to a 0.25° grid.

3. Operational Soil Moisture Data Sets

3.1 ERA40 Re-Analysis Data

The ERA40 re-analysis data set (Simmons and Gibson [2000]) comprises the period from mid-1957 to 2001 overlapping the earlier ECMWF re-analysis ERA15 (1979-1993). The data assimilation system uses the Integrated Forecast System (IFS) at T159 spectral resolution in the horizontal, which corresponds to a 1.125˚ grid point resolution, and 60 vertical levels. The surface scheme within the IFS is the Tiled ECMWF Scheme for Surface Exchanges over Land (TESSEL, van der Hurk et al. [2000]). For ERA40 cycle 23r4 is used, which was operational from June, 12, 2001 to January, 22, 2002. The data sets involved in the re-analysis comprise various satellite observations as well as ground based observations. Data were assimilated using the three dimensional variational assimilation scheme developed by ECMWF. For a complete description of the ERA40 project, the IFS and the validation of the ERA40 surface scheme the reader is referred to www.ecmwf.int/research/era/Project/index.html, www.ecmwf.int/research/ifs/ and van den Hurk et al. [2000], respectively.

ERA40 volumetric soil moisture is obtained for 4 different soil layers: 0-7 cm, 7-28 cm, 28-100 cm and 100-289 cm. Wilting point, field capacity and saturation are prescribed with 0.171, 0.323 and 0.472 m^3/m^3, respectively, and are uniform for the vertical and constant for the entire globe. In this study, the top layer data for 12:00 UTC (universal time coordinated) are interpolated to a 0.25° resolution grid using thin plate splines (Barrodale et al. [1993], Powell [1992]) (Fig. 7). Due to the coarse original resolution of 1.125 ˚ small scale features as the intensive storm at El Reno are not represented by the ERA40 data set. However, the large scale structure with the wet northern part and the drier south is well captured.

3.2 ERS Scatterometer Data

The ERS scatterometer is a 5.3 GHz radar with a spatial resolution of ~ 50 km. Data are available for the period from 1991 to 1996 (ERS-1) and 1995 to present (ERS-2). Over land, the measured backscattering coefficient depends on soil moisture, surface roughness, vegetation characteristics and the incidence angle. In the reviewed literature many studies exhibited high correlations between soil moisture and the backscattering coefficient for bare soil surfaces (Ulaby et al. [1982]). However, correcting for vegetative effects, roughness effects and changing incident angles is a challenging task. Wagner [1998] developed an operational soil moisture retrieval scheme, which takes these effects into account. A global soil moisture data base at 0.25° resolution covering the period from 1992 to 2000 is available through www.ipf.tuwien.ac.at/radar/ers-scat/home.htm.

As stated earlier, microwave radiation interacts with the top few centimeters of the soil. Consequently, only surface soil moisture can be obtained by microwave remote sensing. The standard product of the ERS soil moisture data base is the soil water index (SWI) for the top 100 cm of the soil, which is derived from surface soil moisture (ms). In this study the m_s data set is analyzed since the accuracy of the spatially and vertically integrated SWI product is severely limited by the irregular sampling period, which is caused by the small swath width (500 km) of the ERS scatterometer and the fact that the scatterometer can not be operated in parallel mode with the SAR. In the next paragraph a brief description of the ERS m_s product is given following Wagner [1998].

The algorithm for the ERS surface soil moisture retrieval is based on multi-year time series of scatterometer data. In principle, the retrieval is a change detection method where the actual backscattering coefficient is compared to the lowest backscattering coefficient and the highest backscattering coefficient available at a

given location at corresponding viewing angles. The resulting soil moisture m_s is a relative measure of the moisture content in the top few centimeters. Under the assumption that the lowest and highest backscattering coefficients represent completely dry and saturated soils, respectively, m_s is the degree of saturation and soil porosity can be used to infer volumetric soil moisture. However, the driest possible soil moisture state in nature is always larger than zero and less than the wilting point due to hygroscopic and structural water in the soil. In theory, saturation is the wettest possible condition. Since there will be always some air trapped in the soil (Hillel [1980]), the wettest state observed is expected to be between saturation and field capacity. The transformation of the ERS soil moisture product to volumetric soil moisture is therefore a difficult task, which is beyond the scope of this paper. As a consequence, it is difficult to quantify the systematic errors from the comparison with the PSR data (section 4.2). For the comparison described in section 5 the m_s data were normalized using field capacity and wilting point, which resulted in an almost bias free data set when compared to the in-situ observations.

4. Comparisons between PSR soil moisture and operational products

The previous sections showed that PSR observations are well suited for soil moisture retrievals for the SGP99 experiment. The comparisons with in-situ measurements and the L-band derived soil moisture product suggest that the PSR derived soil moisture product represents the actual state well. To decide whether a future operational soil moisture data set from AMSR has the potential to improve current operational products data from PSR are compared to the ERA40 data set and the ERS product.

Soil moisture is highly variable in space and time. Therefore, soil moisture data sets derived from different sources of information are difficult to compare. In this study, data sets with spatial resolutions ranging from ~500 m to ~120 km have to be compared. The temporal resolution is either a snapshot for the ERA40 and ERS m_s products or a composite image taken over 2.5 hours (PSR). Since the in-situ soil moisture measurements presented in Fig. 2 show a smooth dry down comparisons between data sets taken at different times during a particular day should not be critical. The differences in spatial and horizontal resolution have to be discussed in more detail.

As outlined in section 2, the retrieval of the PSR soil moisture product relies on the brightness temperatures, effective soil temperature, vegetation water content and soil bulk densities based on Landsat TM and the STASGO Data Base. Each data set is characterized by a specific horizontal resolution. In general, the aggregation of geophysical parameters will introduce errors since radiative transfer is a non-linear process. However, for L- and C-band these aggregation errors are small for areas with sparse vegetation characterized by water contents below 1.5 kg m^{-2} (Drusch et al. [1999], Crow et al. [2001]). Aggregating the high resolution PSR soil moisture field to a 0.25° product does not introduce errors. Although the variability in the soil moisture field is reduced the characteristic features of the spatial distribution remain present. In addition, the rainfall distribution at 0.25° exhibits the large scale pattern and the storm in the El Reno area. For the comparison with the ERA40 data it would be best to aggregate the PSR product to 1.125 °. Since the experiment region is too small to get reliable values for this resolution, the ERA40 data were interpolated to a 0.25° grid. This product does not contain any small scale features and shows a much smaller dynamical range of soil moisture values.

The vertical resolution of the PSR and ERS data sets depends on the penetration depth of C-band radiation, which is a function of soil moisture. Therefore, it is almost impossible to assign a number to the depth of the layer, which is actually monitored. Since penetration depth increases for dry soils, the depth of the observed soil layer should vary between ~0.5 and ~3 cm (Ulaby et al. [1982]). The top soil layer in TESSEL has a

depth of 7 cm. In wet conditions, especially immediately after a rainfall event, the NWP model will exhibit lower soil moisture contents than the C-band product. During the dry down event, water will infiltrate into deeper layers and evaporate from the surface layer. Consequently, the 7 cm product will contain more water than the C-band estimate, although the penetration depth of C-band radiation increases.

4.1 PSR vs. ERA40

For the comparison with the PSR data set ERA40 data were interpolated to 0.25° resolution (Fig. 7). The north-south gradient in soil moisture is the most dominant feature in the images. Compared to the PSR data set the dynamic range in the ERA40 soil moisture product is significantly smaller. Although the coarser resolution and the larger soil depth of the top layer should damp the variability in soil moisture it is very likely that the dynamical range of soil moisture in the model predictions is too small. Similar problems with very dry and sandy soils occurred in assimilation experiments with TESSEL using the SGP97 data set (Seuffert et al. [2003a]).

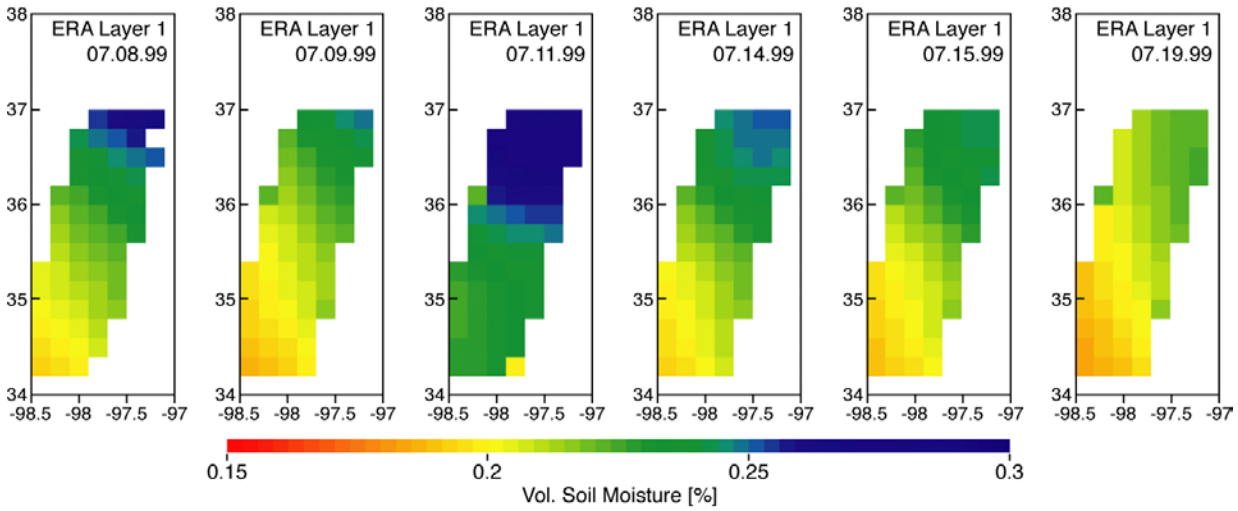

Figure 7 . ERA 40 volumetric soil moisture for the top soil layer (0 – 7 cm) at 12:00 UTC.

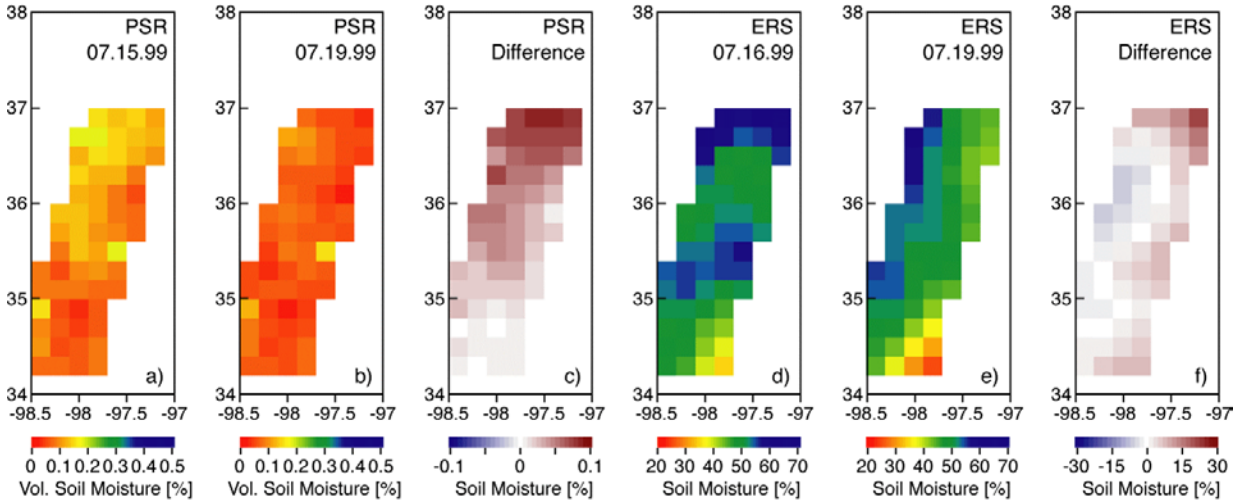

Figure 8 Re-sampled 0.25° grid data for SGP99: a) PSR derived volumetric soil moisture for July 15. b) PSR derived volumetric soil moisture for July 19. c) Differences of PSR derived soil moisture between July 15 and July 19. d) ERS derived m_s for July 16. e) ERS derived m_s for July 19. f) Difference of ERS derived m_s between July 16 and July 19.

A more detailed comparison of the two data sets is given in Fig. 9. For the dates where significant spatial gradients in soil moisture were present correlations ranging from 0.37 to 0.58 for both data sets are obtained. The rms errors vary between 6.4 % and 14.4 %. These are consistently higher values than the rms errors found for the ESTAR and PSR derived soil moisture data sets. During the dry periods at the end of the experiments no correlation between the PSR data and the ERA40 soil moisture product was found. While the north south gradient is still present in the ERA40 data on July 19, no distinct pattern can be observed in the PSR derived soil moisture. It is very likely that this difference in both soil moisture products is related to the different vertical resolutions. The sampling depth of the PSR instrument at that time is ~ 3 cm while the ERA40 first soil layer comprises the top 7 cm. The in-situ measurements for the top 5 cm indicate a north-south gradient when CF and LW stations are compared. The bias in the ERA40 data set increases with decreasing mean soil moisture. After dry periods with corresponding low soil moisture values on 07/09/99 and 07/19/99, the biases are 13.5 % and 14.2 %, respectively. One day after the rainfall events on July 10, the bias was reduced to 3.8 %. The slopes of the regression lines indicate that PSR derived soil moisture is higher in wet conditions and lower in dry conditions when compared to ERA40, which can be explained by the different spatial resolutions and the associated lower dynamical range in the ERA40 soil moisture product. Shortcomings in the model or its parameters may have a contribution as well.

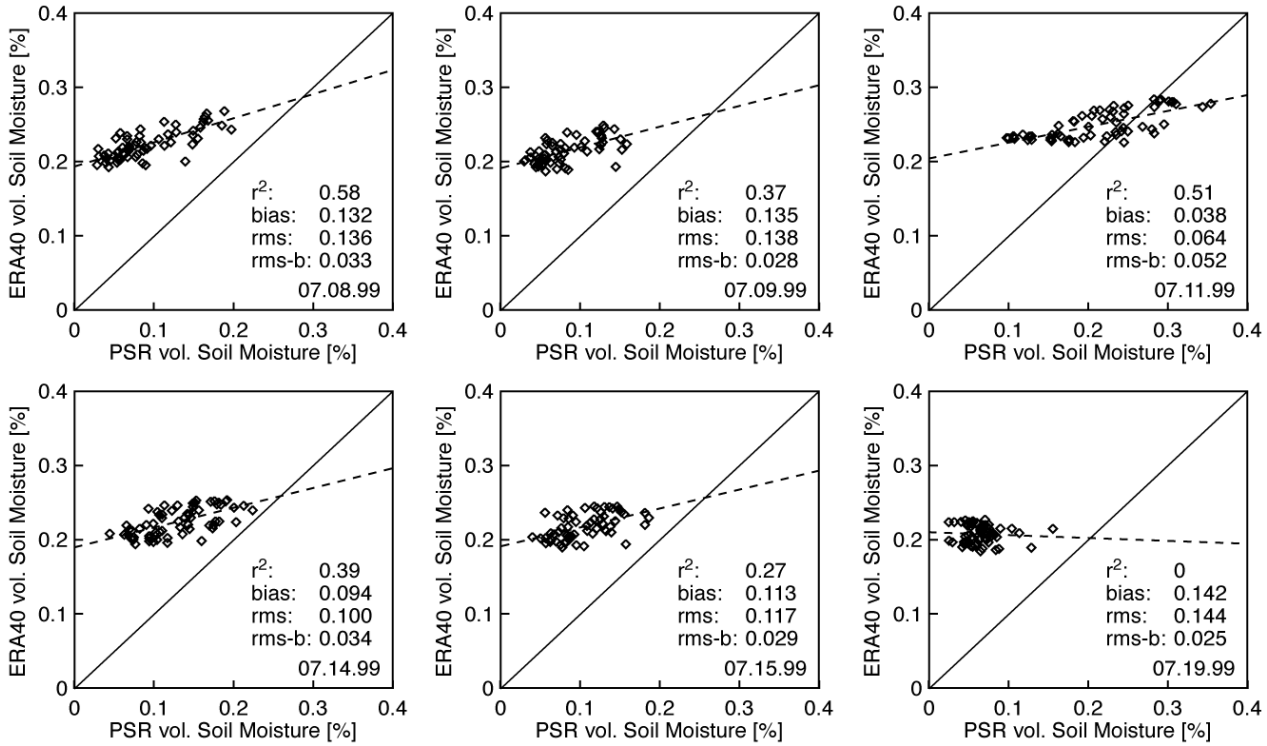

Figure 9 Comparison between volumetric soil moisture derived from PSR brightness temperatures and ERA40 re-analysis soil moisture (7 cm top layer). Data are re-sampled to a 0.25° grid.

These results show very clearly that the hydrological model has problems to predict the soil moisture evolution for the experiment period correctly. With bias corrected rms errors (rms-b) varying from 2.5 % to 5.2 % volumetric soil moisture and a dynamical range in soil moisture of ~10 %, it can be concluded that three states of soil moisture (dry, normal, wet) may be distinguished in the ERA40 product.

4.2 PSR vs. ERS

The analysis of the m_s data set showed that two snapshots with full data coverage for the SGP experiment were available for July 16 and 19 (Figs. 8d and 8e). Since m_s can not directly be converted to volumetric soil moisture a qualitative comparison will be made. The image obtained for July 16 exhibits the north-south gradient with a local minimum north of 36˚ northern latitude (Fig. 8d). Since no PSR or ESTAR data are available for this particular day, the m_s image is compared to the PSR data from the previous day, July 15 (Fig. 8a). An r^2 value of 0.28 was obtained. The corresponding value for the ERA40 product is 0.27. The absolute values for that particular day for m_s vary between ~38 % to ~68 % while the field measurements yield values between ~ 9 % and ~ 19 % volumetric soil moisture. The ERS soil moisture image for July 19 (Fig. 8d) exhibits an east-west gradient, which is neither present in the PSR product (Fig. 8b) nor in the ESTAR data sets. A comparison between PSR and the ERS surface soil moisture results in an r^2 value of 0.14. The spatial variations of m_s range from ~32 to ~58 %, which indicate soil water contents slightly below average. The PSR derived soil moisture map exhibits values from ~2 % to ~15 % volumetric soil moisture, which is at the very dry end of the dynamic range. These values are more realistic for the prevailing synoptic situation. Although the systematic difference between the ERS data set and the experimental data sets is difficult to quantify these results suggest a wet bias in the ERS data for dry scenes. When the ERS m_s image is compared to the vegetation water content derived from NDVI (Jackson et al. [2002]) a correlation coefficient of -0.45 is found. This may be explained by the fact that the sensitivity of the backscattering coefficient to soil moisture is significantly reduced for vegetation covered dry soils (Ulaby et al., [1982]).

5. Comparisons for the NOAA/ATDD site at LW02

The comparisons presented in the previous sections are based on a limited number of dates, which comprise one dry down event. To investigate the accuracy of the operational data sets for a longer period soil moisture measurements at 10 cm depth at the NOAA/ATDD station (Little Washita site no. 2 (34 58’ N, 97 57’ W)) from June 1997 until December 1998 are analyzed. The soil at this site is classified as clay loam, which consists of 25 % sand, 45 % silt and 30 % clay. Figure 10 shows a time series of in-situ measurements, m_s derived from ERS and modeled top layer soil moisture from the ERA40 data set. From both operational data sets, ERA40 and ERS m_s, the nearest grid point was selected for the comparison. Since the ERS m_s product is defined as volume of water per volume of pores, it is not directly comparable to the volumetric soil moisture values presented in Fig. 10. Due to the different spatial resolutions of the three data sets, a quantitative comparison is difficult. An intense storm over the LW area (e.g. at the beginning of July 1997) results in saturated conditions at the field scale, but affects soil moisture at the ERA40 resolution to a much smaller extent. In contrast, rainfall events within an ERA40 grid box may by-pass the LW02 site (e.g. mid of July 1997). In general, ERA40 and ERS m_s capture the dry periods in June, July and August. A more quantitative evaluation of the ERA40 and ERS data sets is shown in Fig. 11. Only dates where all three data sets are available were processed. For this comparison, ERS m_s was converted to volumetric soil moisture using a permanent wilting point of 0.1 m^3/m^3 and a saturation of 0.472 m^3/m^3. The values are reasonable for the prevailing soil types, but it should be noted that slightly different values will change the bias between the in-situ measurements and the ERS data.

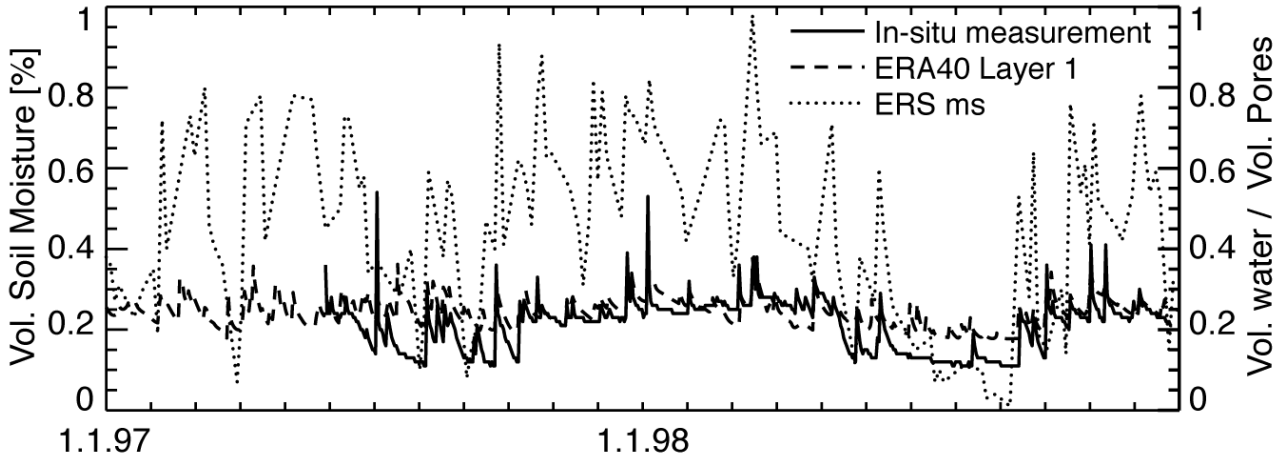

Figure 10 Time series of volumetric soil moisture (volume of water per volume of soil) for the NOAA/ATDD station at LW02: in-situ measurements at 10 cm depth (solid line) and ERA40 top 7 cm layer (dashed line). The ERS m_s (volume of water per volume of pores) is shown as dashed dotted line.

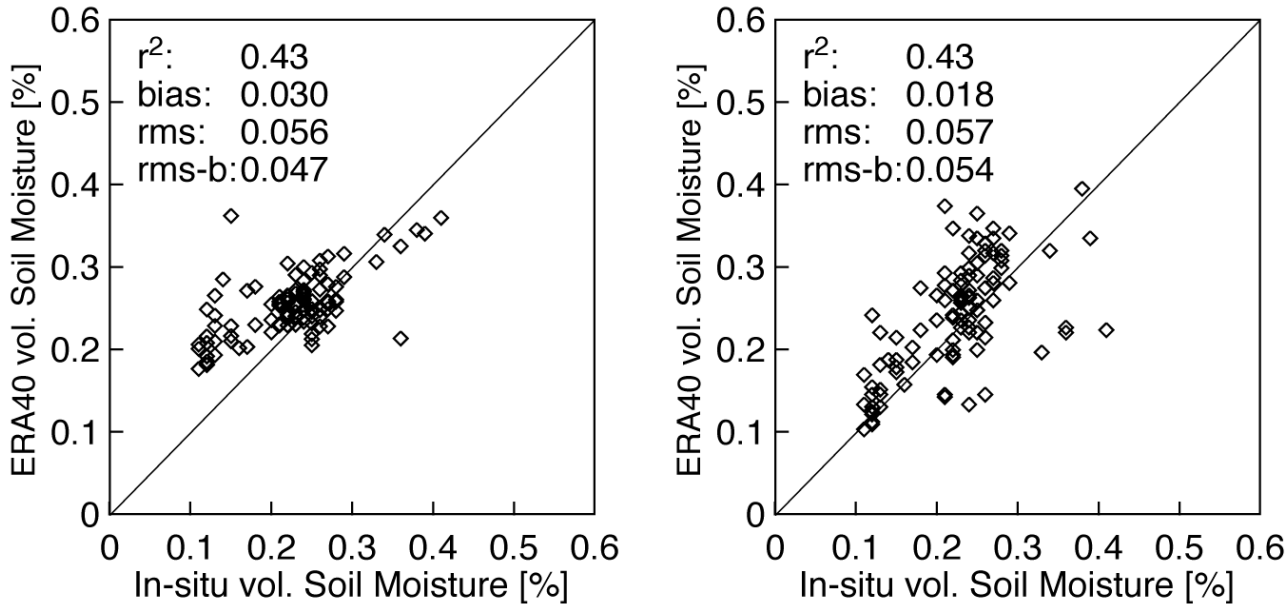

Figure 11 Comparison between in-situ volumetric soil moisture at 10 cm depth and ERA40 (left side) and ERS converted m_s.

Both operational data sets are in good agreement with the observations. Due to the differences in the spatial scale an explained variance r^2 of 0.43 is reasonable. The slightly positive bias in the ERA40 data set is again due to limitations in the model and its soil parameters. The ERA40 data set was derived with one global set of soil parameters and the values given in section 3.1 are certainly not representative for the SGP study region.

6. Summary and Discussion

In this study soil moisture maps were derived from airborne passive microwave L-band and C-band measurements. In contrast to previous studies (Jackson et al. [1999] and Jackson et al. [2002]) *h* and *b* parameters, which determine soil roughness and vegetative effects, are average values taken from a

consistent set of measurements (Schmugge and Jackson [1992]). The in-situ measurements of soil moisture were used as a validation data set. It was found that both data sets can monitor soil moisture on the regional scale with an rms-b error and a bias of ~ 3 %.

The good results obtained for the PSR data set were derived for a sparsely vegetated region after RFI contaminated data were removed (Jackson et al. [2002]). The potential for soil moisture retrievals from C-band over areas with denser vegetation is limited. Ahmed [1995] found that ‚…for NDVIs greater than 0.45 the resultant microwave signal is substantially affected by vegetation'. In addition, the comparison between both data sets indicates the limits of field measurements for calibration and validation. Even for a fairly homogeneous region as the Southern Great Plains, a small bias can be present although the retrieval perfectly matches the observations.

The systematic difference between the ERA40 re-analysis soil moisture of the top layer and the PSR derived field is much larger than 3 %. Values exceeding 14 % were found for the SGP99 experiment during the dry periods. In addition, the random error (rms-b) in the ERA40 is approximately one third of the dynamical range. The experiment domain and period are certainly too limited to fully evaluate the ERS m_s soil moisture product or the retrieval method itself. For the SGP99 experiment period, the irregular sampling interval of ERS was too large to capture the significant wet and dry periods. Within the 14 days only two snapshots of the SGP region with full data coverage were taken. The soil moisture data obtained for July 16 are in reasonable agreement with the spatial distribution prevailing during the previous days. A comparison with the PSR derived soil moisture fields suggests a wet bias in the m_s product for July 19. The results shown in section 5 indicate that the ERS derived surface soil moisture product is as accurate as the re-analysis data set. These findings are in good agreement with other studies (www.ipf.tuwien.ac.at/radar/ers-scat/home.htm). However, the future ASCAT scatterometer will have a double swath width of 2 × 500 km, which will ensure a more frequent data coverage.

Since L-band data from passive microwave instruments will not be available before 2006 (SMOS), C-band measurements from AMSR and ERS / ASCAT are the most promising data sources for the near future. Although the airborne radiometers mimic operational satellite-borne sensors the results from field experiments may not be exactly the same as for AMSR measurements. However, previous studies based on SMMR 6.6 GHz support the findings of this study. SMMR 6.6 GHz data were compared either with soil moisture measurements or antecedent precipitation indices. For Belarus a correlation coefficient of -0.68 between horizontally polarized brightness temperature and in-situ data was found (Lindau et al. [2002]). Ahmed [1995] compared brightness temperatures with a modeled antecedent precipitation index and obtained correlations ranging from 0.6 to 0.89 for the mid-west and southern United States. From the results presented and earlier studies it seems to be realistic that the accuracy goal of at least 6 % for volumetric soil moisture retrievals can be achieved in areas without strong RFI contamination.

It is not clear yet, how these observation errors act in different assimilation schemes (e.g. Seuffert et al. [2003a, 2003b], Reichle et al. [2001a, 2001b]) and different applications. Seuffert et al. [2003a] present an assimilation study with a simplified extended Kalman Filter, the single column version of TESSEL and high quality forcing data. Brightness temperatures, relative humidity and 2m air temperature were assimilated simultaneously. In this experiment set up an rms error exceeding 6 % would be too high to have an impact, since the model error and the errors in screen level parameters are much smaller. In areas, where the quality of the meteorological forcing data is poor and/or no additional observations are available, an accuracy of ~ 6 % can be sufficient. Using the SGP97 data set it was shown that the assimilation of L-band brightness

temperatures corrects for more than 50 % of model error in root-zone (40 cm) soil moisture and latent heat flux predictions associated with the use of temporally sparse rainfall measurements as forcing data (Crow [2003]).

Acknowledgments

The authors would like to thank P. Viterbo (ECMWF) for providing the ERA40 Re-analysis data and K. Scipal (University of Vienna) for providing the relevant data from the ERS soil moisture data base. We also wish to thank T. Jackson and the SGP99 participants for collecting, preparing and distributing the comprehensive SGP99 data sets. The in-situ measurements from the NOAA/ATDD site were provided by T. Meyer. We acknowledge receipt of the OK Mesonet data. The work benefited from discussions with W. Wagner (Univ. of Vienna), E. Andersson (ECMWF), P. Viterbo (ECMWF), T. Hollingsworth (ECMWF) and comments from two anonymous reviewers.

This work was partly funded by the BMBF through the German Climate Research Project DEKLIM (01LD0006).

References

Ahmed, N.U., Estimating soil moisture from 6.6 GHz dual polarization, and/or satellite derived vegetation index, Int. J. Rem. Sens., 16, 687-708, 1995

Barrodale, I., et al., Note: Warping digital images using thin plate splines, Pattern Recognition, 26, 375-376, 1993

Bindlish, R., W.P. Kustas, A.N. French, G.R. Diak, and J.R. Mecikalski, Influence of Near-Surface Soil Moisture on Regional Scale Heat Fluxes: Model Results Using Microwave Remote Sensing Data from SGP97, IEEE Trans. Geo. Rem. Sens., 39, 1719-1728, 2001

Choudhury, B.J., T.J. Schmugge, A. Chang, and R.W. Newton, Effect of surface roughness on the microwave emission of soils, J. Geophys. Res., 84, 5699-5706, 1979

Choudhury, B.J., T.J. Schmugge, and T. Mo, A parameterization of effective temperature for microwave emission, J. Geophys. Res., 87, 1301-1304, 1982

Crow, W.T., Correcting land surface model predictions for the impact of temporally sparse rainfall rate measurements using an Ensemble Kalman Filter and surface brightness temperature observations, J. Hydromet., in press 2003

Crow, W.T., M. Drusch and E.F. Wood, Effects of land surface heterogeneity on AMSR-E soil moisture retrieval, IEEE Trans. Geo. Rem. Sens., 39 (8), 1622 – 1631, 2001

Drusch, M., E.F. Wood, and C. Simmer, Up-scaling effects in passive microwave remote sensing: ESTAR 1.4 GHz measurements during SGP97, Geo. Res. L., 26, 879-882, 1999

Hillel, D., Introduction to Soil Physics, Academic Press, San Diego etc., 365 p, 1980

Jackson, T.J., T.J. Schmugge and J.R. Wang, Passive microwave remote sensing of soil moisture under vegetation canopies, Water Res. Res., 18, 1137-1142, 1982

Jackson, T.J. and T.J. Schmugge, Vegetation effects on the passive microwave emission of soils, Rem. Sens. Env., 36, 203-212, 1991

Jackson, T.J., D.M. Le Vine, C.T. Swift, T.J. Schmugge, and F.R. Schiebe, Large area mapping of soil moisture using the ESTAR passive microwave radiometer in Washita'92, Rem. Sens. Env., 53, 27-37, 1995

Jackson, T.J., D.M. Le Vine, A.Y. Hsu, A. Oldak, P.J. Starks, C.T. Swift, J.D. Isham, and M. Hakan, Soil Moisture Mapping at Regional Scales Using Microwave Radiometry: The Southern Great Plains Hydrology Experiment, IEEE Trans. Geo. Rem. Sens., 37, 2136-2151, 1999

Jackson, T.J. and A.Y. Hsu, Soil Moisture and TRMM Microwave Imager Relationships in the Southern Great Plains 1999 (SGP99) Experiment, IEEE Trans. Geo. Rem. Sens., 39, 1632-1642, 2001

Jackson, T.J., A.J. Gasiewski, A. Oldak, M. Klein, E.G. Njoku, A. Yevgrafov, S. Christiani, and R. Blindish, Soil Moisture Retrieval Using the C-Band Polarimetric Scanning Radiometer During the Southern Great Plains 1999 Experiment, IEEE Trans. Geo. Rem. Sens., 40, 2151-2161, 2002

Joseph, J.H., W.J. Wiscombe and J.A. Weinman, The Delta-Eddington approximation for radiative flux transfer, J. Atm. Sci., 33, 2452-2459, 1976

Kerr, Y.H. and E.G. Njoku, A Semiempirical Model for Interpreting Microwave Emission from Semiarid Land Surfaces as Seen From Space, IEEE Trans. Geo. Rem. Sens., 28, 384-393, 1990

Kerr, Y.H., P. Waldteufel, J.-P. Wigneron, J.-M. Martinuzzi, J. Font, and M. Berger, Soil Moisture Retrieval from Space: The Soil Moisture and Ocean Salinity (SMOS) Mission, IEEE Trans. Geo. Rem. Sens., 39, 1729-1735, 2001

Le Vine, D.M., A.J. Griffis, C.T. Swift, and T.J. Jackson, ESTAR: A synthetic aperture microwave radiometer for remote sensing applications, Proc. IEEE, 82, 1787-1801, 1994

Le Vine, D.M., T.J. Jackson, C.T. Swift, M. Hakan, and S.W. Bidwell, ESTAR Measurements During the Southern Great Plains Experiments (SGP99), IEEE Trans. Geo. Rem. Sens., 39, 1680-1685, 2001

Lindau, R., C. Simmer, and T. Mikhnevich, Soil moisture detection from satellite, BALTEX Newsletter, No. 4, GKSS Forschungszentrum, Geesthacht, Germany, 9-11, 2002

Margulis, S.A., D. Mc Laughlin, D. Entekhabi, and S. Dune, Land Data Assimilation and Estimation of Soil Moisture Using Measurements from the Southern Great Plains 1997 Experiment, Water Res. Res., 38, 10.1029/2001WR001114, 2002

Powell, M.J.D., Tabulation of thin plate splines on a very fine two dimensional grid, Report No. DAMTP 1992/NA2, University of Cambridge, Cambridge, UK, 1992

Reichle, R.H., D.B. McLaughlin, and D. Entekhabi, Variational Data Assimilation of Microwave Radiobrightness Observations for Land Surface Hydrology Applications, IEEE Trans. Geo. Rem. Sens., 39, 1708-1718, 2001a

Reichle, R.H., D. Entekhabi and D.B. McLaughlin, Downscaling of radiobrightness measurements for soil moisture estimation: A four-dimensional variational data assimilation approach, Water Res. Res., 31, 2353-2364, 2001b

Schmugge, T.J. and T.J. Jackson, A Dielectric Model of the Vegetation Effects on the Microwave Emission from Soils, IEEE Trans. Geo. Rem. Sens., 30, 757-760, 1992

Seuffert, G., H. Wilker, P. Viterbo, M. Drusch and J.-F. Mahfouf, On the usage of screen-level parameters and microwave brightness temperature for soil moisture analysis, accepted for publication J. Hydromet., 2003a

Seuffert, G., P. Viterbo, J.-F. Mahfouf, H. Wilker, M. Drusch and J.-C. Calvet, Soil moisture analysis combining screen-level parameters and microwave brightness temperatures: A test with field data, Geophys. Res. Let., 30 (10), 1498, doi:10.1029/2003GL017128, 2003b

Simmons, A.J. and J.K. Gibson, The ERA-40 Project Plan, ERA-40 Project Report Series No. 1, ECMWF, Reading, UK, 63 pp.

Ulaby, F.T., R.K. Moore, and A.K. Fung, Microwave Remote Sensing Active and Passive, Vol. II (Radar Remote Sensing and Surface Scattering and Emission Theory), Artech House, Norwood, MA, US, 1064 pp, 1982

Van den Hurk, B.J.J.M., P. Viterbo, A.C.M. Beljaars and A.K. Betts, Offline validation of the ERA40 surface scheme, Technical Memorandum 295, Research Department, European Centre for Medium-range Weather Forecasts, Reading, 2000.

Wagner, W., Soil Moisture Retrieval from ERS Scatterometer Data, Geowissenschaftliche Mitteilungen Heft 49, Studienrichtung Vermessungswesen, Technische Universität Wien, Wien, 1998.

Wagner, W., J. Noll, M. Borgeaud, and Helmut Rott, Monitoring Soil Moisture over the Canadian Prairies with the ERS Scatterometer, IEEE Trans. Geo. Rem. Sens., 37, 206-216, 1999

Wagner, W. and K. Scipal, Large-Scale Soil Moisture Mapping in Western Africa Using the ERS Scatterometer, IEEE Trans. Geo. Rem. Sens., 38, 1777-1782, 2000

Wang, J.R. and T.J. Schmugge, An empirical model for the complex dielectric permittivity of soils as a function of water content, IEEE Trans. Geo. Rem. Sens., 18, 288-295, 1980